Coexistence of meandering and bunching of steps on vicinal surfaces

Yan-Mei Yu[1,2] and Bang-Gui Liu[3,1,2]
[1]*Institute of Physics, Chinese Academy of Science, P.O. Box 603, 100080 Beijing, China*
[2]*Beijing National Laboratory for Condensed Matter Physics, Beijing 100080, China*
[3]*Department of Physics, University of California, Berkeley, California 94720, USA*
(Received 26 May 2005; revised manuscript received 2 September 2005; published 9 January 2006)

We simulate morphology and its evolution of vicinal surfaces in epitaxy by using the phase-field model. For usual parameters of Cu vicinal surfaces, a pure in-phase meandering pattern consistent to the experimental images is obtained. Nevertheless, vicinal surfaces grow into more complex hierarchy for a small kink energy. In addition to step meandering, step bunching happens due to competition of local step fluctuation and interlayer Ehrlich-Schwoebel barrier in the presence of the step meandering. This implies that step meandering and step bunching can coexist in some growing epitaxial vicinal surfaces.

DOI: 10.1103/PhysRevB.73.035416 PACS number(s): 81.15.Aa, 68.35.Fx, 68.35.Ct

I. INTRODUCTION

It has been recognized for several decades that steps play the central role to help achieve layer-by-layer growth of atomically flat thin films. Recently, the step flow growth in the limit far from equilibrium is actively explored as a promising alternative approach for planar nanostructures on surfaces. Straight steps on a vicinal surface are usually unstable under the condition of being far from equilibrium. The steps either become wavy in the mode of step meandering (SM),[1–4] or remain straight but become closer to each other in some regions and more separate in the others in the mode of step bunching (SB).[5,6] Experimentally and theoretically, SM and SB were considered to be exclusive during epitaxial growth, and therefore, one-dimensional (1D) models are enough to study SB of straight steps[7,8] and SM of a single step.[3] However, Neel *et al.*[9] reported recently that on vicinal Cu(100) surfaces SB develops with SM as the precursor and the bunched steps remain wavy. The experimental two-dimensional (2D) morphology indicates that a more realistic model is needed for describing such steps on vicinal surfaces.

We use a 2D model to describe real steps on growing vicinal surfaces. We simulate the evolution and morphology of such 2D steps by using a phase-field approach.[10–12] This approach allows us to obtain a fine visualized morphology of epitaxial vicinal surfaces in the 2+1 dimensions. Asymmetric inter-terrace Ehrlich-Schwoebel (IES) effect along steps makes the steps unstable against meandering during growth. An in-phase SM appears on the vicinal substrates. Local SB can result from fluctuations of neighboring steps for small kink energy. Neighboring monatomic steps bunch into a super structure of steps. The SB, interacting with the in-phase SM, can produce local broad terraces where islands can nucleate and grow into some three-dimensional (3D) mounds subsequently. Our phase-field simulation shows that SM and SB can coexist during epitaxial growth on some vicinal surfaces.

II. PHASE-FIELD MODEL OF EPITAXIAL GROWTH ON VICINAL SURFACES

We construct the phase-field model by introducing a continuum phase-field variable Φ and a local adatom variable. $\Phi=0,1,2,\ldots$, and n describe sequentially the bottom terrace, the first terrace, the second terrace, …, and the nth terrace. The sharp steps between different terraces in atomic models are described by the spatial transition zone (STZ) of the phase field, which can be identified by nonzero $\nabla\Phi$. We formulate the time and space variation of Φ in terms of the equation[10]

$$\frac{\partial\Phi}{\partial t}=\frac{1}{\tau}[\nabla W^2\nabla\Phi-2\sin 2\pi\Phi-2\lambda(\cos 2\pi\Phi-1)u]+\lambda_n u^2, \tag{1}$$

where parameter W is a phase-field parameter, τ is a kinetic parameter, and λ is a dimensionless coupling constant. The local adatom variable is defined by $u=(c-c_{eq})\Omega$, where c is local adatom concentration, Ω is the atomic area (a^2 for square lattice of lattice constant a), and c_{eq} is the equilibrium concentration at a straight step. The potential term of the free energy is formulated as a periodic function of Φ so that it takes degenerate local minimums for $\Phi=0,1,2,\ldots,n$, and, when $u>0$, these minimums decrease with Φ increasing. We add the term $\lambda_n u^2$ to consider the nucleation of islands. The exponent 2 comes from the assumption that the critical size of the islands is 1.

The local variable u obeys the equation

$$\frac{\partial u}{\partial t}=\nabla D\nabla u-\frac{\partial\Phi}{\partial t}+\Omega\delta(\vec{r}-\vec{r}\,')\delta(t-t'), \tag{2}$$

where D is the diffusion coefficient of adatoms, whose dimension is m^2/s. After the length is scaled by a, as we do in the simulations, the dimension of D is $1/s$. The first term on the right hand side (rhs) describes diffusion of adatoms, and the second one the depletion of adatoms for island growth. The third term describes the deposition of adatoms. This term reduces to F, the deposition rate of adatoms, if being averaged along the time and on the substrate area S. To simulate real deposition, $\vec{r}\,'$ is randomized, and t' is discretized with the time interval being given by Ω/FS. D is equivalent to $D_0=\Omega\nu\exp(-E_d/k_BT)$ on terraces, where ν is the attempt frequency, E_d the diffusion barrier, k_B the Boltzmann constant, and T the temperature. D is modified in the STZ re-

 ©2006 The American Physical Society

gions. The STZ region can be divided into two parts: upward one identified by positive $\nabla^2\Phi$, and downward one identified by negative $\nabla^2\Phi$. We reduce D gradually from the terraces to the upward STZ centers in order to imitate the weak terrace-climbing motion of adatoms. In the downward STZ, we modify D into $D_{es}=D_0\exp(-E_s/k_bT)$ in order to imitate the suppression of the Schwoebel barrier E_s on downward motion of adatoms. In the thin interface limit, Eqs. (1) and (2) reduce to the BCF model except for the nucleation term and the randomness of the deposition term.

We define $W(\theta)=W_0a_s(\theta)$ to simulate the anisotropy, where angle θ denotes the step's local normal direction. According to the Wulff-plot of the step free energy on fcc(100) surfaces,[13] we write

$$a_s(\theta) = 1 + \eta\cos[4(\theta - \theta_0)], \tag{3}$$

where $\eta \in [0,1]$ measures the magnitude of the anisotropy, and θ_0 denotes the angle between the normal direction of the step of the largest step free energy and the reference direction. The phase-field parameters W_0, τ, and λ in Eq. (1) are determined by the physical parameters at steps according to the following two equations obtained by the thin-interface asymptotic analysis[11]

$$\lambda = \frac{a_1 k_B W_0 T}{a^2 c_{eq}\gamma_0} \quad \text{and} \quad \tau = \frac{a_1 a_2 k_B W_0^3 T}{a^2 D c_{eq}\gamma_0}, \tag{4}$$

where c_{eq} is determined by the barrier, E_{ad} for adatoms escaping from kinks onto terraces according to $c_{eq}=\exp(-E_{ad}/k_BT)$. The constants a_1 and a_2 take 0.36 and 0.51 by means of thin-interface asymptotic analysis in terms of the free energy function in Eq. (1).[10,11] γ_0 is the isotropic step stiffness, which is determined by the kink energy ε at steps according to $\gamma_0=k_BT\exp(\varepsilon/k_BT)/2a$. The excess free energy for the phase-field interface can be calculated from first derivative of stationary solution of the phase field. Equation (1), with $W(\theta)$ included, implies an anisotropic step stiffness.[11] The relation of W_0 and γ_0 also is explicitly shown in Eq. (4).

Equations (1) and (2) are solved in a square domain, of 200×200 by using the second order finite differential method on a uniform Cartesian grid, and by using the first order finite differential approximation in the time domain. Initializing Φ on the square, we construct a vicinal substrate, where monatomic steps are in the x direction, forming a step train of the spacing eight along the y direction. When the substrate is subtracted, we can use periodic boundary condition for Φ and u in both directions. A new adatom is deposited on terraces one by one. In the simulations the length is scaled by a, and we choose $W_0=2$ and the grid spacing $\Delta x=1$. Being far less than the characteristic length of the step morphology or our substrate size 200, the thickness of the STZ is less than $6\Delta x$ for these parameters, which allows for the qualitative simulation. Therefore we expect that the phase-field simulated images represent the detailed structure of the step morphology. $\theta_0=0°$ is chosen for the vicinal surface of (001) terraces separated by open $\langle100\rangle$ steps, and $\theta_0=45°$ is for the vicinal surface of (001) terraces and closed-packed $\langle110\rangle$ steps. We choose $\eta=0.06$, which indicates $\gamma_{\langle100\rangle}/\gamma_{\langle110\rangle}=1.13$. Referring to the corresponding values for the Cu(100) homoepitaxial system,[13] we choose $E_d=0.40$ eV, $E_{ad}=0.35$ eV, $E_s=0.052$ eV, $\nu=10^{12}$, and $\varepsilon=0.126$ eV for a simulation with $T=250$ K and $F=0.1$ ML/s. The other simulation is conducted for a reduced ε of 0.025 eV. The parameter λ_n describes the nucleation rate, which is proportional to D for epitaxy systems.[10] We choose $\lambda_n=20$ for our simulations. This means a mediate nucleation rate that cannot cause island nucleation on narrow interstep terraces, but can yield island nucleation on wide interstep terraces.

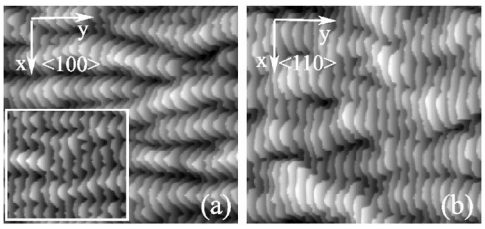

FIG. 1. The simulated morphology on the vicinal substrate with the kink energy $\varepsilon=0.126$ eV. The temperature is $T=250$ K, the flux $F=0.1$ ML/s, and the coverage 20 ML. The anisotropy of the step free energy is considered for the vicinal surface consisting of (001) terraces and $\langle100\rangle$ steps (a) and for that of (001) terraces and $\langle110\rangle$ steps (b). Inset is the earlier step morphology when the coverage is 5 ML.

III. PHASE-FIELD RESULTS OF STEP INSTABILITY ON VICINAL SURFACES

The simulated images are shown in Figs. 1 and 2. As mentioned above, we design a spatially-changing D for the stepped structure as shown in the inset in Fig. 2(a), which corresponds to a positive IES barrier. The steps are unstable

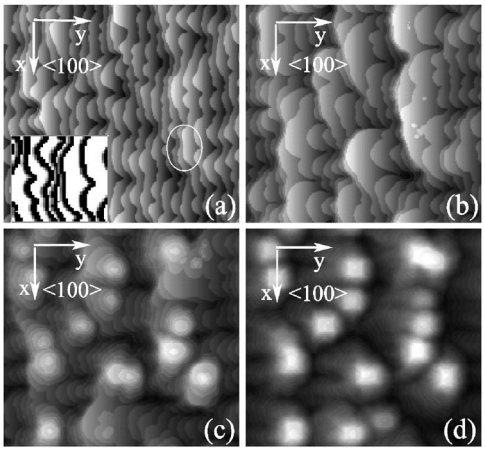

FIG. 2. The evolution of the morphology on the vicinal substrate with coverage increasing. The parameters are the same as Fig. 1, but the kink energy is equivalent to $\varepsilon=0.025$ eV. The coverage is 5, 10, 15, and 20 ML in (a)–(d), respectively. The inset is an enlarged display of modified diffusion on the region denoted by the circle. The white, gray, and black correspond to terrace, upward STZ, and downward STZ, respectively.

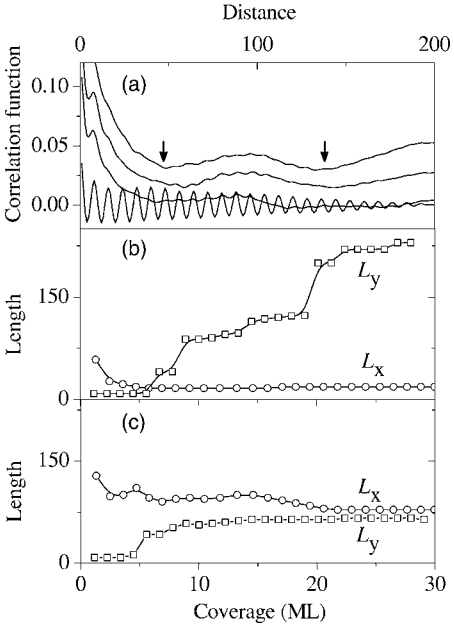

FIG. 3. The height correlation of the growing surface as functions of coverage. (a) shows the height correlation functions in the y direction obtained for different coverages of 1, 10, 14 and 16 ML, corresponding to plots from down to up for $\varepsilon=0.126$ eV. (b) shows the characteristic lengths, L_x and L_y, for $\varepsilon=0.126$ eV, and (c) for $\varepsilon=0.025$ eV.

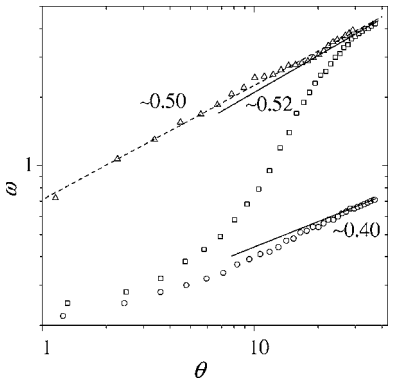

FIG. 4. Root mean square fluctuation widths of the steps and surface, ω, versus the coverage θ (in units of monolayer). The step fluctuation width (triangle) and surface fluctuation width (circle) are for the kink energy $\varepsilon=0.126$ eV, and the surface fluctuation width (square) for $\varepsilon=0.025$ eV. The dash line is the linear fit of $\omega \sim \theta^{0.50}$ and the two solid lines denote the power laws $\omega \sim \theta^{0.52}$ and $\omega \sim \theta^{0.40}$.

against meandering during growth. They evolve into "sharp-angled" protrusions in the case of $\theta_0=0°$ and "square-angled" protrusions in the case of $\theta_0=45°$. In both cases, the growing steps are mostly oriented along the $\langle 110 \rangle$ direction which corresponds to the smallest step free energy. The meandering steps grow with equal spacings, forming the in-phase morphology eventually, as shown in Fig. 1. Inset in Fig. 1(a) shows the step morphology in the early stage. The simulated images resemble closely those observed on homogenous Cu(100) vicinal substrates.[9] The scaling law of the wavelength of the in-phase meandering is $(D/F)^{\alpha}$ with $\alpha=0.3\pm0.04$. This exponent is in between 1/2 of Bales-Zangwill mechanism[1] and 1/4 in the presence of kink ES (KES) barrier and edge diffusion.[2,4,14] SM also appears in the simulation of $\varepsilon=0.025$ eV. However, it is surprising that local SB occurs in front of some meandering steps, as shown in Fig. 2. The bunched steps remain wavy in a larger space scale, which yields broad terraces. Islands nucleate on these terraces and grow into multilayer mounds. This is another instability of the growing surface in addition to the step instability.

To quantify these results, we consider height correlation function of the epitaxy overlayers. With the substrate being subtracted from the surface, local height is described by $\zeta(\vec{r})=\zeta(\vec{r})-\bar{\zeta}$, where $\bar{\zeta}$ is its spatial average. The correlation function along a unit vector $\vec{v}$ is defined by $H_{\vec{v}}(l)=1/S\int d\vec{r}\zeta(\vec{r})\zeta(\vec{r}+l\vec{v})$, where S is the substrate area. Figure 3(a) illustrates the evolution of $H_y(r)$ with θ increasing for the simulated results with $\varepsilon=0.126$ eV. We estimate the characteristic length L_x in the x direction and L_y in the y direction by averaging the valley-valley and/or peak-peak distances in $H_x(r)$ and $H_y(r)$. The evolution of L_x and L_y is illustrated in Figs. 3(b) and 3(c) for $\varepsilon=0.126$ eV and $\varepsilon=0.025$ eV, respectively. In Fig. 3(b) L_x remains a constant value, indicating the characteristic wavelength of the in-phase SM, while the stepwise-increasing L_y indicates persistent extension of the in-phase property along the step train. In Fig. 3(c) L_x almost remains constant for $\theta<15$ ML, describing the lateral separation of step bunches, and it decreases a little with θ increasing for larger θ, indicating nucleation of islands. The small variation of L_x and L_y indicates limited coarsening of mounds on the stepped structures.

In Fig. 4 shown is the root mean square (rms) fluctuation widths of the steps and surface as functions of θ. In the case of $\varepsilon=0.126$ eV the step fluctuation width increases according to $w \sim \theta^{0.50}$. This is consistent with $w \sim \sqrt{t}$ predicted in terms of a nonlinear dynamic equation.[3] The surface fluctuation width increases with θ, following a power law $w \sim \theta^{0.40}$. In the case of $\varepsilon=0.025$ eV, the simultaneous existence of SM, SB, and islands causes large variation of the surface fluctuation width. First, the w increases slowly when the step growth is dominated by SM for $\theta<3$ ML. Then, the w increases rapidly because of the SB. Finally, the island growth overruns upon the step growth, resulting in roughening of the surface. Here we obtain the scaling law $w \sim \theta^{0.52}$, as is shown in Fig. 4. The exponent is consistent with experimental roughening exponent 0.2–0.5 for Cu(100) singular surface.[15] As is shown in Figs. 3 and 4, the height correlation functions for $\varepsilon=0.126$ and $\varepsilon=0.025$ are characterized respectively as two different growth modes: (1) the pure in-phase SM and (2) the coexistence of SM, SB, and island growth. The evolution of the fluctuation widths shown in Fig. 4 indicates that these growths reach their stationary regime eventually.

IV. MECHANISM OF STEP INSTABILITY

Our simulation reveals that growth and relaxation compete. When a fast attachment kinetic at steps is assumed, "growth" is driven by the adatoms captured at the steps,

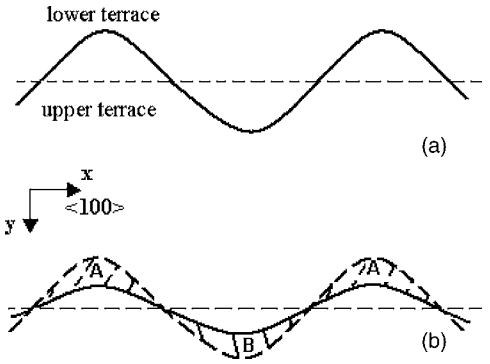

FIG. 5. A schematic figure for the origin of the mass flux along the steps. The x and y directions are consistent with the above figures. (a) shows a wavy step, and (b) shows the mass transport from the peak to the valley, or from the A part to B part, which yields an effective mass transport along the steps (the x direction) in addition to the mass transport across the steps (the y direction).

which is described by the term $\lambda(\cos 2\pi\Phi - 1)u$ in Eq. (1). Because the adatoms captured at the steps come from the terraces, the capture is diffusion limited. Because of the D modification at the vicinity of steps the protruding segments capture more adatoms and then progress faster. The diffusivity on the terrace edges at peaks is reduced by the D modification, compared with that on the terrace edges at valleys. This yields a mass transport from valleys to peaks. This effect is effectively equivalent to the effect of the KES barrier on the edge diffusion along steps. On the other hand, the variation of the step profile causes Gibbs-Thomson (GT) effect which is included in the phase-field model implicitly. The GT effect smoothes the wavy steps through driving the adatoms from peaks to valleys in terms of the u diffusion term $\nabla D \nabla u$ in Eq. (2). This causes an asymmetric diffusion between the peaks and valleys, and yields effectively a mass transport along the step edge (that is, x) direction, as Fig. 5 shows. Therefore, this explains why our D/F scaling exponent of the wavelength of the in-phase meandering is in between $1/2$ of IES mechanism and $1/4$ of KES mechanism. At the same time, this effect makes the local density of adatoms change by the meandering of the surrounding steps, causing a long-range correlation of the step growth. In this way, the long-range effect is included in our simulation while considering the atomic kinetics. This correlation makes fluctuation of neighboring steps be in phase and explain why the steps are unstable against the in-phase meandering for $\varepsilon = 0.126$.

The correlation of the step growth becomes weak in the case of $\varepsilon = 0.025$ because of the reduced step stiffness. Before the in-phase dynamics become dominant, arbitrary fluctuation at each step makes some segments of neighboring steps move closer. It happens more likely in front of large protrusions because these protrusions progress faster, approaching the steps in front of them, as denoted by the circle in Fig. 2(a). The IES effect is relatively weak on the broad top terraces of the large protrusions, which allows them to persist growing fast. As a result, more steps bunch together in front of the large protrusions. But when a balance has been established between the adatoms captured at the large protrusions and those at the hind steps, the progress of the large protrusions slows down and then SB stops growing.

There are at most 5–6 steps in a step bunch. The terrace width l persists decreasing during the step growth, being independent of the total number of steps, N, in the bunch. There is no scaling law of l vs N. This is in contrast with SB in Cu(100) system at high temperature, which follows a scaling law $l \propto N^{-0.29}$. The difference is made by the fact that our simulation is conducted for the step growth at low temperatures. At high temperatures the KES barrier may be a key contribution to SM,[9,14] whereas the IES barrier is of an ignorable role for SM. The anisotropic edge diffusion under the KES barrier is proposed to originate from SB at high temperature for Cu(100) system.[16] Whether local SB for a small kink energy occurs at high temperatures for the KES barrier needs to be made clear in future work. Driven by electric currents, Si(111) vicinal surface could develop into morphology with both SB and SM.[17–20] In contrast, the coexistence of SB and SM in the Cu(100) vicinal surface is induced by asymmetric barriers across steps. The two systems need different mechanisms, which can be seen in their morphologies.

V. CONCLUSION

In summary, we simulate the instability of 2D steps on vicinal surfaces by using the phase-field model. Relating the local atomic kinetics to the long-range correlation, the phase-field simulations show dependence of the step instability on the kink energy. The pure in-phase meandering instability is obtained in the case of a Cu(100) kink energy, whereas locally step bunching happens in the meandering steps for a smaller kink energy as a result of competition of step fluctuation determined by long-range correlation and local atomic kinetics.

ACKNOWLEDGMENTS

This work is supported by the Chinese Department of Science and Technology under the National Key Basic Research Program (No. 2005CB623602), by the Nature Science Foundation of China (Nos. 60021403 and 10134030), and by the Berkeley Scholars Program, University of California, Berkeley, CA 94720.

[1] G. S. Bales and A. Zangwill, Phys. Rev. B **41**, 5500 (1990).
[2] O. Pierre-Louis, M. R. D'Orsogna, and T. L. Einstein, Phys. Rev. Lett. **82**, 3661 (1999).
[3] O. Pierre-Louis, C. Misbah, Y. Saito, J. Krug, and P. Politi, Phys. Rev. Lett. **80**, 4221 (1998).
[4] M. Rusanen, I. T. Koponen, J. Heinonen, and T. Ala-Nissila, Phys. Rev. Lett. **86**, 5317 (2001).
[5] R. L. Schwoebel, J. Appl. Phys. **40**, 614 (1968).
[6] F. Liu and H. Metiu, Phys. Rev. E **49**, 2601 (1994).
[7] A. Pimpinelli, I. Elkinani, A. Karma, C. Misbah, and J. Villain, J. Phys.: Condens. Matter **6**, 2661 (1994); A. Pimpinelli, V. Tonchev, A. Videcoq, and M. Vladimirova, Phys. Rev. Lett. **88**, 206103 (2002).
[8] P. Politi, G. Grenet, A. Marty, A. Ponchet, and J. Villain, Phys. Rep. **324**, 271 (2000).
[9] N. Neel, T. Maroutian, L. Douillard, and H. J. Ernst, Phys. Rev. Lett. **91**, 226103 (2003); T. Maroutian, L. Douillard, and H. J. Ernst, Phys. Rev. Lett. **83**, 4353 (1999); Phys. Rev. B **64**, 165401 (2001).
[10] Y.-M. Yu and B.-G. Liu, Phys. Rev. E **69**, 021601 (2004); Phys. Rev. B **70**, 205414 (2004).
[11] A. Karma and W. J. Rappel, Phys. Rev. Lett. **77**, 4050 (1996); A. Karma and M. Plapp, Phys. Rev. Lett. **81**, 4444 (1998).
[12] O. Pierre-Louis, Phys. Rev. E **68**, 021604 (2003).
[13] M. Giesen, Prog. Surf. Sci. **68**, 1 (2001).
[14] J. Kallunki, J. Krug, and M. Kotrla, Phys. Rev. B **65**, 205411 (2002).
[15] H. J. Ernst, F. Fabre, R. Folkerts, and J. Lapujoulade, Phys. Rev. Lett. **72**, 112 (1994); J.-K. Zuo and J. F. Wendelken, *ibid.* **78**, 2791 (1997).
[16] P. Politi and J. Krug, Surf. Sci. **446**, 89 (2000).
[17] M. Suzuki, Y. Homma, Y. Kudoh, and R. Kaneko, Ultramicroscopy **42-44**, 940 (1992).
[18] H. Minoda, I. Morishima, M. Degawa, Y. Tanishiro, and K. Yagi, Surf. Sci. **493**, 487 (2001).
[19] D. Kandel and J. D. Weeks, Phys. Rev. Lett. **74**, 3632 (1995).
[20] M. Sato, M. Uwaha, and Y. Saito, Phys. Rev. B **62**, 8452 (2000).